



## A GEANT-based package for determination of the *Pamir* experiment X-ray emulsion chamber response

A.S. BORISOV<sup>a</sup>, V.G. DENISOVA<sup>a</sup>, V.I. GALKIN<sup>b</sup>, M.G. KOGAN<sup>a</sup>, E.A. KANEVSKAYA<sup>a</sup>,  
K.A. KOTELNIKOV<sup>a</sup>, R.A. MUKHAMEDSHIN<sup>c\*</sup>, S.I. NAZAROV<sup>b</sup>, V.S. PUCHKOV<sup>a</sup>

(a) *Lebedev Physical Institute, Moscow, 119991 Russia*

(b) *Skobel'tsyn Institute of Nuclear Physics, Moscow, 119992 Russia*

(c) *Institute for Nuclear Research, Moscow, 117312 Russia*

\*[muhamed@sci.lebedev.ru](mailto:muhamed@sci.lebedev.ru)

**Abstract:** The *ECSim* 2.0 package version is released aimed at simulation of the development of nuclear-electromagnetic cascades initiated by different particles in stratified media with a particular attention paid to a response of X-ray emulsion chambers. Features of *ECSim* 2.0 and results of simulation are discussed for the case of the passage of electrons and  $\gamma$ -rays through the  $\Gamma$ -block of *Pamir* experiment X-ray emulsion chambers.

### Introduction

The *ECSim* 2.0 package version is intended for detailed 3D-simulation of development of nuclear-electromagnetic cascades (NEC) initiated by different particles, from protons to nuclei, in X-ray emulsion chambers (XREC) on the basis of GEANT 3.21 package. It is based on the *ECSim* 1.0 [1] used by RUNJOB experiment which, however, cannot be directly applied to the simulation of the ground-based experiments detecting secondary particles ( $\pi$ ,  $K$  etc.). The *ECSim* 2.0 code can be used in a broader field of problems for simulations of NECs in complex and multi-layer media in a wide range of energies from 10 keV to  $\sim 100$  PeV accounting for specific measuring procedures exploited in XREC experiments. This paper is devoted to the simulation of the *Pamir* experiment XREC response.

### Simulation of particle propagation processes through XREC

The *ECSim* v. 2.0 package incorporates:

- the LPM effect for electromagnetic processes (following version 1.0);
- generation of hadron-hadron and hadron-nucleus

interactions at  $E > 80$  GeV using the QGSJET model [3] (following version 1.0);

- simulation of NECs initiated in the chamber by hadrons of various types ( $p/\bar{p}$ ,  $n/\bar{n}$ ,  $\pi$ ,  $K/\bar{K}$  and so on),  $e^\pm$ ,  $\gamma$ -rays at different incident angles (new feature);
- tracking of correlated groups of particles ( $\gamma$ ,  $e^\pm$ ,  $h$ ) of high energy ( $E \gtrsim 4$  TeV), the so-called  $\gamma$ - $h$  families, passing through XREC that requires substantial changes in the logic of processing of these events (new feature);
- simulation of the passage of superhigh-energy muons with appropriate cross sections for bremsstrahlung,  $e^+e^-$  pair production, knock-on electron production and nuclear interaction similar to those used in GEANT4 (new feature);
- accounting for the LPM effect which appreciably decreases the pair production cross section at high enough energies ( $E \gtrsim 70$  TeV) in the case of high-Z lead absorber, the most frequently used one in XREC structures; respectively, the muon cross section was reduced by a factor proportional to the  $\gamma$ -ray cross section decrease at the same energy (new feature);
- LPM-corrected cross sections for bremsstrahlung by electrons and pair production by  $\gamma$ -rays were extended up to  $10^{19}$  eV energies (new feature).

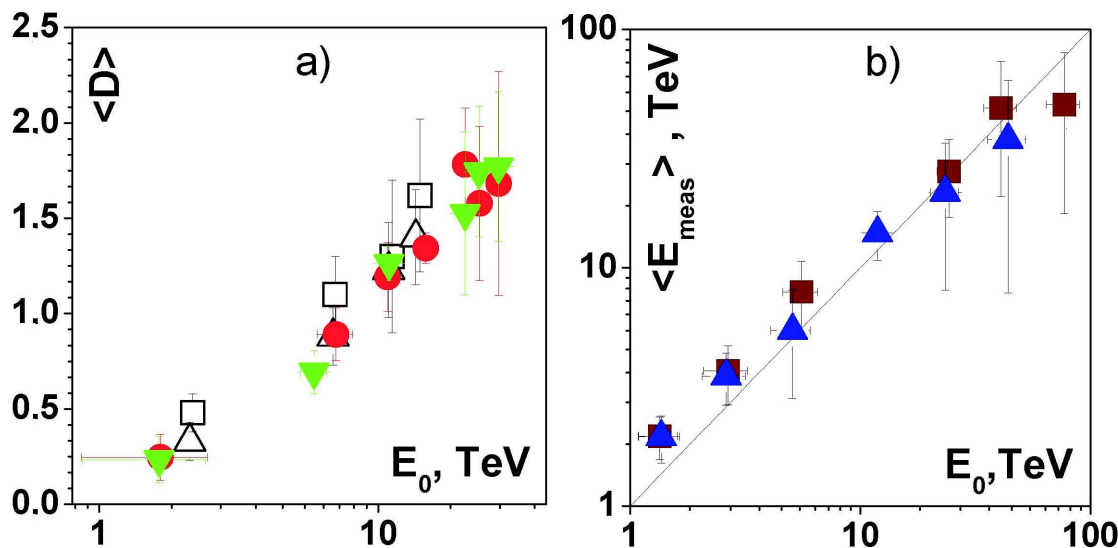


Figure 1: (a) Average optical density  $\langle D \rangle$  dependence on primary energy  $\langle E_0 \rangle$  at 9-r.l. depth for  $\gamma$ -rays (circles) and electrons (triangles), incident angles are  $15^\circ \leq \theta \leq 25^\circ$ . Empty squares and triangles are the data of [2] for  $e/\gamma$  flux with incident angles  $0^\circ \leq \theta \leq 5^\circ$  and  $15^\circ \leq \theta \leq 25^\circ$ , respectively, at 9-r.l. depth. (b) Average "measured" energy  $\langle E_{\text{meas}} \rangle$  dependence on primary energy  $E_0$  of electrons (squares) and  $\gamma$ -rays (triangles) at 9-r.l. depth, incident angles are  $0^\circ \leq \theta < 12^\circ$ . Straight line is the case  $\langle E_{\text{meas}} \rangle = E_0$ .

*ECSim 2.0* makes it possible to analyze the NEC development in any stratified medium. Test results show good agreement with other authors' data. For instance, the  $n_{ch}$  transition curves in Pb in cascades initiated by  $\gamma$ -rays of energy  $E_0 = 1$  PeV and traced down to  $E_{\text{min}} = 1$  TeV agree with results [4].

### Simulation of darkening spot formation

One of the most important points of XREC technique is the measurement of darkness of spots produced on X-ray films by electron-photon cascades (EPC) and corresponding reconstruction of EPC energies. To simulate the darkness measurement procedure, the field of view of the measuring diaphragm (aperture) is divided into square cells of linear size  $l_{\text{cell}}$ . The *Pamir* experiment used measuring diaphragms with radii  $R_d \simeq 48 \div 140 \mu\text{m}$ . A relation used by the *Pamir* experimenters for calculation of darkness density is  $D = D_0 \{1 - \exp(-s\rho)\}$ . Here  $s = 3.25 \pm 0.13 \mu\text{m}^2$ ,  $\rho$  is the number of particles per unit square.

While charged particles cross the emulsion plane, their number  $N_i$  in  $i$ th cell is summed up and recorded, and the darkness  $D_i$  is calculated according to the above-given relation. For all  $K$  cells visible within the aperture of a given shape and size, the total "measured" darkness  $D_{\text{tot}}$  is calculated as follows

$$D_{\text{tot}} = \lg K - \lg \sum_{i=1}^K 10^{-D_i(N_i)}.$$

Particularly, this approach enables to reproduce the conventional *Pamir* procedure for darkness measurement by circular diaphragms of a given radius  $R_d$ . The calculated  $D_{\text{tot}}$  value makes it possible to evaluate the cascade energy applying the standard *Pamir* procedure for determination of the EPC energy on the basis of the measured darkness.

It is important to optimize the cut-off energy  $E_{\text{min}}$  for cascade secondary particle tracing. It was shown that the cut-off optimal value is  $E_{\text{min}} = 1$  MeV. Lower values do not improve the simulation accuracy but do increase the simulation time.

What follows are simulations of the *Pamir* experiment XREC  $\Gamma$ -block which incorporates 5 cm (9 r.l.) of lead with two double-layer X-ray films be-

neath as well as calculations of darkening spots produced by cascades traversing the X-ray films.

The gap between the lead surface and underlying film sensitive layer was taken to be  $500 \mu\text{m}$ , and  $l_{cell} = 16 \mu\text{m}$  was set for the cell size within diaphragm inner region while smaller  $l_{cell}$  values were applied to the diaphragm near-to-boundary ring.

### Single particle detection

The measuring of single electromagnetic particle ( $e^\pm, \gamma$ ) spectra was simulated. It was assumed that incident particles were distributed over energy according to a power-law differential spectrum of power index  $\gamma = -3.0$ . Their angular distribution was assumed to be of the form  $dN/d\Omega \sim \cos^6 \theta$  within the zenith angle domain  $0^\circ < \theta \leq 36^\circ$ .

Fig. 1(a) shows simulation results for the average optical density  $\langle D \rangle$  vs. primary energy  $E_0$  at  $R_d = 48 \mu\text{m}$  for electrons and  $\gamma$ -rays. One can see that these data agree well with the results [2] at  $R_d = 50 \mu\text{m}$ .

Figs. 1(b) and 2 present the data obtained while averaging over three diaphragm radii ( $R_d = 48, 84,$  and  $140 \mu\text{m}$ ).

Fig. 1(b) shows the average "measured" energy  $\langle E_{meas} \rangle$  at 9-r.l. depth versus primary energy  $E_0$ . The standard *Pamir* procedure of energy reconstruction is seen to work well at  $E_0 = 4 - 70 \text{ TeV}$ . At  $E_0 > 70 \text{ TeV}$  the procedure underestimates the "measured" energy for both  $\gamma$ -rays and electrons but the effect is more pronounced for  $\gamma$ -rays. This is due to the fact that the standard procedure does not take the LPM-effect into account properly. It was also shown that the standard procedure takes proper account of the gaps between the lead plates and films.

Fig. 2 presents "measured" energy spectra. The power-law indices are  $\gamma_{meas}^e = -3.03 \pm 0.06$  for electrons and  $\gamma_{meas}^\gamma = -3.12 \pm 0.04$  for  $\gamma$ -rays. Thus, the "measured" spectra are close to the incident spectra by the slopes but still are slightly steeper due to the above-mentioned incorrect accounting for the LPM effect.

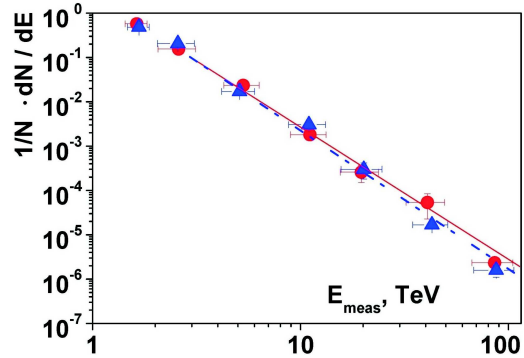


Figure 2: "Measured" energy spectra (averaged over three diaphragm-radius values) of electrons ( $\bullet$ , —) and  $\gamma$ -rays ( $\Delta$ , - - -).

### Correlated groups of particles

While tracking groups of correlated particles ( $\gamma, e^\pm$ , hadrons of so-called  $\gamma$ - $h$  families) through XRECs, one must substantially change the logic of their processing as the total darkness picture in a sensitive layer may be essentially influenced by overlapping of narrow collimated group of particles (induced EPCs to be more precise) inside a family. Spots overlap frequently, especially at higher energies. In this case the following algorithm is applied which reproduces in details the experimental measuring procedure:

- 1) The observation area is divided into cells of size  $l_{cell}$ ; number of charged particles produced in each cell by all EPCs induced by family particles in XREC is calculated.
- 2) While using the simulation data on numbers of particles in cells produced by each of the EPCs (independently of other EPCs), the darkness "measured" by a diaphragm with radius  $R_d$  centered at the cell with maximum number of particles, is calculated for each EPC.
- 3) A procedure of maximization of the "measured" darkness is launched, i.e., the diaphragm center walks around the maximum darkness cell over several (depending on presence of spots) neighboring cells; the "measured" darkness at each step is calculated; the maximum darkness for the diaphragm applied is found.
- 4) For more exact energy determination, the so called "near-by" extra background in the vicinity of each EPC is calculated in accordance with

experimental procedure, i.e., the background produced by all the family EPCs in the neighboring to the given EPC area ( $500 \div 1000 \mu\text{m}$  far from EPC center depending on its energy).

5) A procedure of spot visibility identification (or spot recognition) is applied taking into account two main effects of overlapping of neighboring spots produced by different EPCs.

These effects are as follows: a) overestimation of "measured" energies of close but recognized EPCs; b) spots produced by some EPCs are not visible against the total background or that produced by neighboring EPCs. To avoid these effects, which could essentially distort the calculated results, the following procedure of spot visibility identification has been designed trying to reproduce the experimental situation.

1) Let us consider a spot (hereafter named spot 1) with darkness  $D_1$ . If there is no other spots with darkness  $D_i > D_1$  (measured with a diaphragm  $R_d = 48 \mu\text{m}$ ) at a distance of  $\lesssim 1 \text{ mm}$  from the center of spot 1, then spot 1 is treated as visible. Otherwise the analysis is continued.

2) It is taken that the the spot 1 is seen against the background produced by spot 2 with  $D_2 > D_1$ , if the maximum darkness of spot 1,  $D_{1max}$ , is higher than a minimum darkness  $D_{1-2min}$  ("measured" during the drift toward the center of spot 2) not less than by 30 percent according to the Rayleigh's criterion applied to the spot visibility. In doing so, the procedure searches for  $D_{1-2min}$  by deviating by some distance, which depends on size of spot 1, from the direct line connecting the centers of both spots. The maximum distance restricting the searching area is equal to the minimum one of two values, i.e., either the half distance between the centers of both spots or distance from the spot center to a place where the spot darkness is practically not distinguished against the background. To calculate the spot visibility by the Rayleigh's criterion, diaphragms of different small enough radii ( $R_d \simeq 22 \div 38 \mu\text{m}$ ) are used depending on spot size. Besides, the average darkness is calculated along the line connecting the centers of both spots over the above-defined distance. The spot 1 is treated as invisible due to apparatus restrictions, if this darkness "measured" by the same measuring diaphragm appears to be higher than  $D_{1max}$ .

## Conclusion

The *ECSim* 2.0 package is designed to simulate both the NEC development in complex-structure medium at  $10 \text{ keV} \lesssim E_0 \lesssim 100 \text{ PeV}$  and  $\gamma$ - $h$  family energy measurement procedure applied in XREC experiments.

It is shown that the *Pamir* standard procedure of energy determination by darkness values measured within circular apertures works well at  $E_\gamma = 4-70 \text{ TeV}$ .

## Acknowledgements

This work is supported by the RFBR, projects 05-02-17599, 05-02-16781, 06-02-16606, 06-02-16606, 06-02-16969; and Ministry of Education and Science, projects SS-5573.2006.2, 02.518.11.7084)

## References

- [1] Galkin V.I., Nazarov S.N. Simulation of cosmic ray passage through an emulsion chamber *Preprint SINP MSU* 1999. 99-14/572
- [2] Haungs A. *Nucl. Phys. B* (Proc. Suppl.), 2006. V. 151. P. 215-222.
- [3] Kalmykov N.N. and Ostapchenko S.S. QGS model taking into account jets and EAS *Yad. Fiz.* 58 (1994) 21.
- [4] 02.518.11.7084 Okamoto M., Shibata T. *Nucl. Instrum. & Methods in Phys. Res.* A257 (1987) 155.